

Molecular Pathogenesis of Genetic and Inherited Diseases

# Chronic Oxidative Stress Causes Amplification and Overexpression of *ptprz1* Protein Tyrosine Phosphatase to Activate $\beta$ -Catenin Pathway

Yu-Ting Liu,\* Donghao Shang,<sup>†</sup> Shinya Akatsuka,\* Hiroki Ohara,\* Khokon Kumar Dutta,\* Katsura Mizushima,<sup>‡</sup> Yuji Naito,<sup>‡</sup> Toshikazu Yoshikawa,<sup>§</sup> Masashi Izumiya,<sup>¶</sup> Kouichiro Abe,<sup>¶</sup> Hitoshi Nakagama,<sup>¶</sup> Noriko Noguchi,<sup>||</sup> and Shinya Toyokuni\*

From the Departments of Pathology and Biology of Diseases\* and Urology,<sup>†</sup> Graduate School of Medicine, Kyoto University, Kyoto; Medical Proteomics,<sup>‡</sup> and Inflammation and Immunology,<sup>§</sup> Graduate School of Medicine, Kyoto Prefectural University of Medicine, Kyoto; the Biochemistry Division,<sup>¶</sup> National Cancer Center Research Institute, Tokyo; and the Science and Engineering Research Institute,<sup>||</sup> Doshisha University, Kyoto, Japan

**Ferric nitrilotriacetate induces oxidative renal tubular damage via Fenton-reaction, which subsequently leads to renal cell carcinoma (RCC) in rodents. Here, we used gene expression microarray and array-based comparative genomic hybridization analyses to find target oncogenes in this model. At the common chromosomal region of amplification (4q22) in rat RCCs, we found *ptprz1*, a tyrosine phosphatase (also known as protein tyrosine phosphatase  $\zeta$  or receptor tyrosine phosphatase  $\beta$ ) highly expressed in the RCCs. Analyses revealed genomic amplification up to eightfold. Despite scarcity in the control kidney, the amounts of PTPRZ1 were increased in the kidney after 3 weeks of oxidative stress, and mRNA levels were increased 16~552-fold in the RCCs. Network analysis of the expression revealed the involvement of the  $\beta$ -catenin pathway in the RCCs. In the RCCs, dephosphorylated  $\beta$ -catenin was translocated to nuclei, resulting in the expression of its target genes *cyclin D1*, *c-myc*, *c-jun*, *fra-1*, and *CD44*. Furthermore, knock-down of *ptprz1* with small interfering RNA (siRNA), in FRCC-001 and FRCC-562 cell lines established from the induced RCCs, decreased the amounts of nuclear  $\beta$ -catenin and suppressed cellular proliferation concomitant with a decrease in the expression of target genes. These results demonstrate that chronic oxida-**

**tive stress can induce genomic amplification of *ptprz1*, activating  $\beta$ -catenin pathways without the involvement of Wnt signaling for carcinogenesis. Thus, iron-mediated persistent oxidative stress confers an environment for gene amplification. (Am J Pathol 2007, 171:1978–1988; DOI: 10.2353/ajpath.2007.070741)**

Oxidative stress is associated with a plethora of pathological conditions, including infection, inflammation, UV and  $\gamma$ -irradiation, and overload of transition metals and certain chemical compounds.<sup>1</sup> Many epidemiological studies demonstrated a close association between chronically oxidative conditions and carcinogenesis. Chronic tuberculous pleuritis causes a high incidence of malignant lymphoma<sup>2</sup>; chronic *Helicobacter pylori* infection is associated with a high incidence of gastric cancer<sup>3</sup>; inflammatory bowel diseases are risk factors for colorectal cancer<sup>4</sup>; a high risk for hepatocellular carcinoma is found in patients with genetic hemochromatosis<sup>5,6</sup>; exposure to asbestos fibers rich in iron is frequently associated with mesothelioma and lung cancer<sup>7</sup>; severe burn by UV radiation is a risk factor for skin cancer<sup>8</sup>; and  $\gamma$ -irradiation causes a high incidence of leukemia.<sup>9</sup> As an initiation process under these circumstances and also as a coordinated strategy in proliferating tumor cells,<sup>10</sup> oxidative stress appears to play a role in human carcinogenesis. Thus, an analysis that determines genomic and expressional alterations in an established oxidative stress-induced carcinogenesis is of great importance.

Supported in part by a Grant-in-Aid from the Ministry of Education, Culture, Sports, Science and Technology of Japan, a MEXT grant (Special Coordination Funds for Promoting Science and Technology), a grant of Long-range Research Initiative by Japan Chemical Industry Association, and a Grant-in-Aid for Cancer Research from the Ministry of Health, Labour and Welfare of Japan.

Accepted for publication September 6, 2007.

Address reprint requests to Shinya Toyokuni, M.D., Ph.D., Department of Pathology and Biology of Diseases, Graduate School of Medicine, Kyoto University, Kyoto, Japan. E-mail: toyokuni@path1.med.kyoto-u.ac.jp.

An iron chelate, ferric nitrilotriacetate (Fe-NTA) causes oxidative renal proximal tubular damage via a Fenton reaction that ultimately leads to a high incidence of renal cell carcinoma (RCC) in mice<sup>11</sup> and rats<sup>12</sup> after repeated intraperitoneal administration. This model is intriguing in that 1) more than half of the induced tumors metastasize to the lung and/or invade the peritoneal cavity, resulting in animal mortality<sup>13</sup>; 2) evidence exists for the involvement of free radical reactions in carcinogenesis, including not only covalently modified macromolecules (oxidatively modified DNA bases<sup>14,15</sup> and lipid peroxidation products<sup>16,17</sup>) but also preventive action of  $\alpha$ -tocopherol against carcinogenesis<sup>18</sup>; and 3) genetic changes in *p16<sup>INK4a</sup>* tumor suppressor gene, especially large deletions,<sup>19,20</sup> and expressional alteration of several key genes, including *annexin 2* overexpression<sup>21</sup> and also loss of *thioredoxin-binding protein-2* based on methylation of the promoter region,<sup>22</sup> have been observed.

Here, we performed array-based comprehensive genomic hybridization and gene expression microarray analyses using Fe-NTA-induced rat RCCs and their cell lines to find amplified oncogenes in this model. A common chromosomal amplification at 4q22 in cancers resulted in the discovery of  $\beta$ -catenin pathway activation via gene amplification and overexpression of *ptprz1* protein tyrosine phosphatase.

## Materials and Methods

### Animal Experiments and Chemicals

The carcinogenesis study was performed as previously described<sup>13</sup> using specific pathogen-free male Wistar rats (Shizuoka Laboratory Animal Center, Shizuoka, Japan) or male F1 rats hybrid between Fischer344 and Brown-Norway strains (Charles River, Yokohama, Japan). The animals were kept under close observation and were sacrificed when they showed persistent weight loss and distress. Histological grade of tumor was determined according to the modified World Health Organization classification as we previously described.<sup>13</sup> The animal experiment committee of Graduate School of Medicine, Kyoto University approved this experiment. All of the chemicals used were of analytical quality.

### Array-Based Comparative Genomic Hybridization

We performed array-based comparative genomic hybridization (CGH) with an Agilent 185K rat genome CGH microarray chip (Agilent Technologies, Santa Clara, CA), as described in the Agilent Oligonucleotide Array-based CGH for Genomic DNA Analysis Protocol ver. 4.0, and analyzed results with CGH Analytics Software (ver. 3.4). For each array, normal kidney tissue was used as a reference and labeled with Cy-3. Samples of interest were each labeled with Cy-5.

### *Ptporz1* Genome Copy Analysis

Genomic DNA was extracted with a DNA Extractor WB kit (Wako, Osaka, Japan). A Platinum SYBR Green qPCR SuperMix UDG kit (Invitrogen, Carlsbad, CA) and Real-time PCR system 7300 (Applied Biosystems, Foster City, CA) were used. Primer sequences were as follows, based on NW\_047689: forward, 5'-CCTTACAGGT-GAAAGTCAGC-3'; and reverse, 5'-GGTATACTTTGGC-CCACAGT-3' (130-bp product).

### *Ptporz1* Genome DNA Fluorescent in Situ Hybridization

Three bacterial artificial chromosome clones (CH230–385 M3, CH 230–160 P8, CH 230–418 P21) were extracted with a big bacterial artificial chromosome DNA isolation kit (Princeton Separations, Adelphia, NJ), labeled with biotin-16-dUTP via nick translation (Roche, Tokyo, Japan) and used as probes (2  $\mu$ g/ml) for hybridization in ULTRAhyb hybridization buffer (Ambion, Austin, TX) as previously described.<sup>20</sup> Either formalin-fixed paraffin-embedded sections or cell lines were used on MAS-GP-coated glass slides (Matunami Glass Ind., Ltd., Kishiwada, Japan) after smear preparation.

### Gene Expression Microarray

A total of 10 microarrays (Rat Genome 230 2.0; 31,999 genes; Affymetrix Inc., Santa Clara, CA) were used for screening purpose: two for each group of untreated control, Fe-NTA treatment for 1 week, Fe-NTA treatment for 3 weeks, Fe-NTA-induced RCCs with neither peritoneal invasion nor metastasis, and Fe-NTA-induced RCCs with pulmonary metastasis. Total RNA was isolated with Isogen (Nippon Gene Co. Ltd., Tokyo, Japan), and the degree of gene expression was then evaluated with GeneChip analysis (Focus array; Affymetrix) as previously described.<sup>23</sup> Network analysis was performed using Ingenuity Pathways Analysis (Ingenuity Systems, Redwood City, CA).

### RT-PCR

Total RNA was extracted with TRIzol (Invitrogen), and cDNA was synthesized using RNA PCR kit ver. 3.0 (Takara, Shiga, Japan) with random primers. We then amplified specific cDNA regions for each *ptprz1* isoform with PCR based on a previous report<sup>24</sup> and NM\_013080. Primer sequences were as follows: primer set 1 for A, B, and S forms: forward, 5'-atgcgaatcctgcagagctcc-3', and reverse, 5'-ggtcagcagacacctctttgtac-3' (1723-bp product); primer set 2 for A and S forms: forward, 5'-ggcctcgggtgtttatgaca-3', and reverse, 5'-tgtgtccgaagcagcatgaa-3' (1700-bp product); primer set 3 for A form: forward, 5'-tcagagcctgcgctctctgaca-3', and reverse, 5'-gtcaacagtgcagctctgcact-3' (1745-bp product); and primer set 4 for A and B forms: forward, 5'-ttaggtattacagcagacagctcc-3', and reverse, 5'-tcagactaaagactccag-gctttc-3' (1737-bp product). For quantitative real-time PCR, a Platinum SYBR Green qPCR SuperMix UDG kit

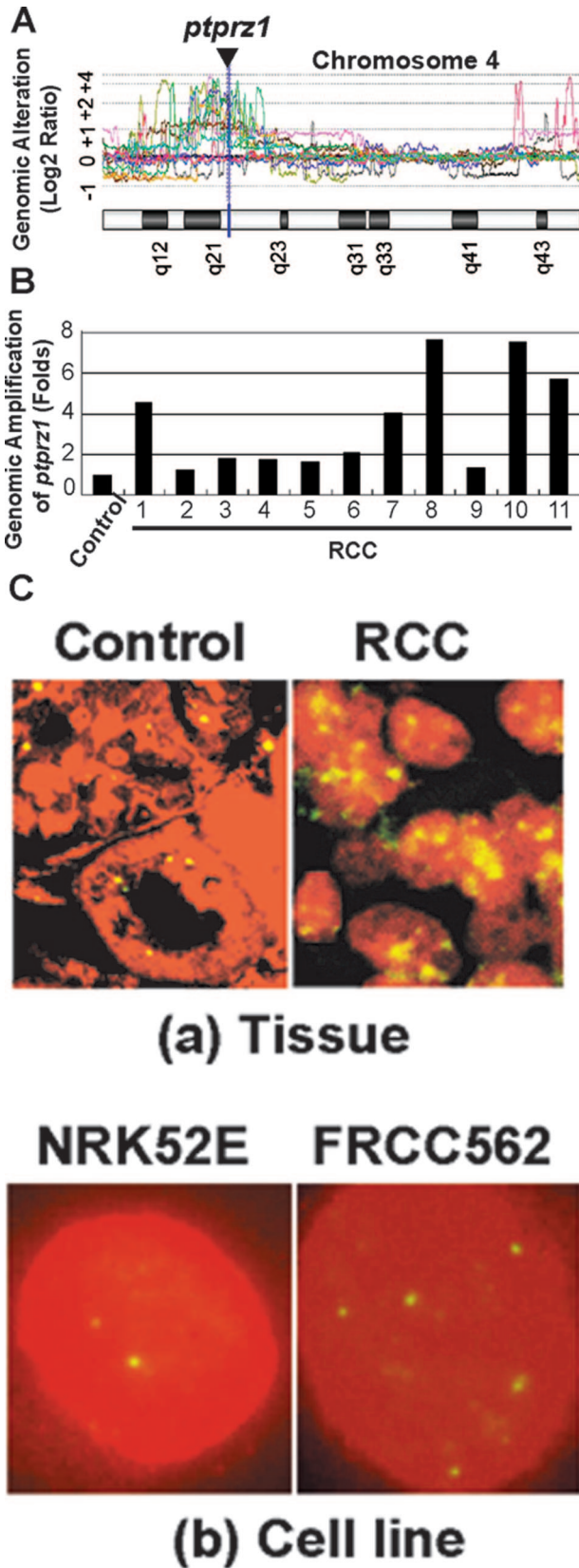


**Figure 1.** Gene amplification of *ptpz1* in Fe-NTA-induced RCCs. **A:** Array-based CGH analysis of 13 Fe-NTA-induced RCCs and 2 established cell lines, with profiles of chromosome 4 showing a broad peak at 4q22. Plus number at y axis indicates amplification at the chromosomal locus (log<sub>2</sub> scale), whereas minus number indicates allelic loss; 0 is the normal 2N-state. Each

(Invitrogen) and Real-time PCR system 7300 (Applied Biosystems) were used. The glyceraldehyde 3-phosphate dehydrogenase gene was used as an internal control as previously described.<sup>23</sup> PCR reactions for each target and control genes were performed in triplicate. Primer sequences used were as follows: *ptpz1* based on NM\_013080: forward, 5'-cccagctgggtggtatgattcc-3', and reverse, 5'-cgtgactttgaagctctctcgcaa-3' (104-bp product); *cyclinD1* based on NM\_171992: forward, 5'-tgtgcatccatgcccggaaa-3', and reverse, 5'-gacaagaaacggtc-caggtagt-3' (114-bp product); *c-myc* based on NM\_012603: forward, 5'-tgtctatttggggacagtggttc-3', and reverse, 5'-ctgttagcgaagctcaggtt-3' (149-bp product); *c-jun* based on NM\_021835: forward, 5'-gtgaaatgacagct-gagtgtctg-3', and reverse, 5'-gtcaacagctctggactgtgg-3' (141-bp product); *fra-1* based on NM\_012953: forward, 5'-ctgctaagtcagaaaaccga-3', and reverse, 5'-caaggcgtctcttctgctt-3' (129-bp product); and *CD44* based on NM\_012924: forward, 5'-tttggtggcacacagcttg-3', and reverse, 5'-atggaatacacctgcgtaacgg-3' (104-bp product).

*Ptpz1* mRNA In Situ Hybridization

Phosphate-buffered formaldehyde-fixed, paraffin-embedded specimens were used as previously described<sup>25</sup> using a DNA probe containing three repeats of ATT (underlined) at the 3' end for T-T dimer formation with an exposure to 10 kJ/m<sup>2</sup> UV irradiation (5'-ctgagtatggcctcaaccagtgctgctgtaagattattatt-3'). Minor modifications include pretreatment with 20 μg/ml proteinase K (37°C, 20 minutes), use of TDM-2 monoclonal antibody for T-T dimer (1:4000 dilution),<sup>26</sup> and an application of tyramide signal amplification biotin system (PerkinElmer Japan, Yokohama, Japan) for sensitive detection.

Cell Culture

Cells were cultured in Dulbecco's modified Eagle's medium (GIBCO, Rockville, MD) containing 5% (NRK52E; Health Science Research Resources Bank, Osaka, Japan) or 10% (FRCC-001 and FRCC-562 cell lines<sup>21</sup>) fetal bovine serum, 100 U/ml penicillin, 100 μg/ml streptomycin, and 0.25 μg/ml amphotericin B at 37°C in a humidified 5% CO<sub>2</sub> incubator.

Expression Vectors and Transfection

Coding sequence of rat *ptpz1* (GenBank accession number NM\_013080) was cloned by RT-PCR using cDNA of normal rat cerebrum as a substrate with the following primers: forward primer, 5'-ggggtaccacccacctggagat-

color shows a different tumor. **B:** Copy number analysis by quantitative PCR. Eleven primary RCCs were analyzed. Means are shown after triplicate measurements that showed within 4% difference. Control, normal untreated kidney. **C:** Fluorescent *in situ* hybridization analysis of *ptpz1* genome. **a:** Paraffin-embedded specimen of Fe-NTA-induced RCC. Control, normal untreated kidney. **b:** Cell lines. Original magnification: ×160 (**a**); ×400 (**b**). Control kidney and NRK52E nontransformed rat renal tubular cell lines showed two or fewer (tissue) signals in the nucleus (nuclear counterstaining by propidium iodide), whereas RCC and FRCC-562 cell line showed more than two signals. Representative images are shown.

**Table 1.** Top 20 Up- and Down-Regulated Genes in Nonmetastatic RCCs

GenBank no.	Gene description	Fold change
Genes up-regulated in nonmetastatic RCCs		
NM_130741	<i>Lipocalin 2 (oncogene 24p3)</i>	3541.1
AW528743	<i>Major histocompatibility complex, class II, DQ <math>\alpha</math>1</i>	282.1
AI137672	<i>CD69 antigen (p60, early T-cell activation antigen)</i>	184.8
AJ249701	<i>RT1 class Ib, locus Aw2</i>	140.1
NM_013080	<i>Protein tyrosine phosphatase, receptor-type, Z polypeptide 1</i>	101.8
NM_012812	<i>Cytochrome c oxidase subunit VIa polypeptide 2</i>	80.4
NM_133311	<i>Interleukin 24</i>	70.0
X73371	<i>Fc fragment of IgG, low affinity IIb, receptor (CD32)</i>	57.7
U05675	<i>Fibrinogen <math>\beta</math>-chain</i>	49.2
NM_133298	<i>Glycoprotein (transmembrane) nmb</i>	46.5
BE101834	<i>Laminin, <math>\beta</math>3</i>	43.7
NM_017222	<i>Solute carrier family 10, member 2</i>	39.9
AB020967	<i>Tribbles homolog 3 (Drosophila)</i>	39.1
NM_016994	<i>Complement component 3</i>	35.5
AI144754	<i>Rho family GTPase 1</i>	34.1
AF413572	<i>Protein kinase inhibitor <math>\beta</math></i>	32.7
NM_022800	<i>Purinergic receptor P2Y, G-protein coupled, 12</i>	30.1
NM_012823	<i>Annexin A3</i>	26.9
NM_030845	<i>Chemokine (C-X-C motif) ligand 2</i>	26.5
NM_013110	<i>Interleukin 7</i>	24.4
Genes down-regulated in nonmetastatic RCCs		
X04280	<i>Calbindin 1, 28 kDa</i>	3769.1
D13906	<i>Aquaporin 2 (collecting duct)</i>	885.3
M27883	<i>Serine peptidase inhibitor, Kazal type 1</i>	471.1
NM_017111	<i>Solute carrier family 21, member 1</i>	455.1
L29403	<i>Potassium inwardly-rectifying channel, subfamily J, member 1</i>	430.5
NM_031703	<i>Aquaporin 3</i>	205.1
J04488	<i>Prostaglandin D2 synthase 21 kDa (brain)</i>	178.5
NM_017082	<i>Uromodulin (uromucoid, Tamm-Horsfall glycoprotein)</i>	176.1
NM_052802	<i>Kidney androgen regulated protein</i>	159.8
NM_017081	<i>Hydroxysteroid (11-<math>\beta</math>) dehydrogenase 2</i>	130.7
NM_016996	<i>Calcium-sensing receptor (hypocalcemic hypercalcemia 1, severe neonatal hyperparathyroidism)</i>	124.5
Z30663	<i>Chloride channel Kb</i>	117.0
BI288461	<i>ATPase, H<sup>+</sup> transporting, lysosomal 56/58 kDa, V1 subunit B, isoform 1 (Renal tubular acidosis with deafness)</i>	113.0
AI235942	<i>Aquaporin 4</i>	112.2
BG377322	<i>Serpin peptidase inhibitor, clade C, member 1</i>	112.2
NM_022676	<i>Protein phosphatase 1, regulatory subunit 1A</i>	111.4
NM_012842	<i>Epidermal growth factor (<math>\beta</math>-urogastrone)</i>	97.7
AF189724	<i>Chemokine (C-X-C motif) ligand 12</i>	94.4
NM_012593	<i>Kallikrein 7 (chymotryptic, stratum corneum)</i>	89.9
NM_013097	<i>Deoxyribonuclease I</i>	81.6

gcgaatcctgca-3' (*KpnI*), and reverse primer, 5'-gggg-gatatccccctaccgtcaggtcatgggaagt-3' (*EcoRV*). PCR products were digested with *KpnI* and *EcoRV* (recognition sequences underlined) and subcloned into a mammalian expression vector pcDEF3,<sup>27</sup> which was transfected into NRK52E cell line with Lipofectamine 2000 (Invitrogen) and selected with 400 to 800  $\mu$ g/ml G418.

### siRNA Experiments

We designed siRNA oligonucleotides through siDirect software.<sup>28</sup> The target *ptprz1* sequence was 5'-AACCC-TATGCACCAACTAGAAA-3' (6819–6841), and the siRNA was as follows: sense oligonucleotide, 5'-CCCU-UAUGCACCAACUAGAAA-3', and antisense, 5'-UC-UAGUUGGUGCAUAAGGGUU-3'. The target  $\beta$ -catenin sequence was gagtcagcgactgttcaaaact (1125 to 1147), and the siRNA was as follows: sense, 5'-GAGUCAGC-GACUUGUUCAAAA-3', and antisense, 5'-UUGAA-

CAAGUCGCUGACUCGG-3'. The negative control (NegC; Naito1) was as follows: sense, 5'-GUACCG-CACGUCUAUUCGUAUC-3', and antisense, 5'-UAC-GAAUGACGUGCGGUACGU-3' (RNAi Co., Ltd, Tokyo, Japan). FRCC-001 and FRCC-562 were seeded in the complete medium without antibiotics to 30 to 50% confluence, transfected with siRNA oligonucleotides with Lipofectamine 2000, and incubated for 48 to 72 hours to confirm gene expression with quantitative RT-PCR and Western blot analysis.

### Fractionation, Immunoprecipitation, and Western blot

These were done as previously described<sup>22,29</sup> except that 0.2 mmol/L Na<sub>3</sub>VO<sub>4</sub>, 50 mmol/L NaF, 1 mmol/L dithiothreitol, and 5.7  $\mu$ g/ml aprotinin were included in the lysis buffer. Antibodies used were as follows: PTPRZ1

**Table 2.** Top 20 Up- and Down-Regulated Genes in Metastatic RCCs

GenBank no.	Gene description	Fold change
Genes up-regulated in metastatic RCCs		
NM_130741	<i>Lipocalin 2 (oncogene 24p3)</i>	2702.4
AI102790	<i>Branched chain aminotransferase 1, cytosolic</i>	1910.9
NM_133514	<i>Matrix metalloproteinase 10 (stromelysin 2)</i>	1112.8
M60616	<i>Matrix metalloproteinase 13 (collagenase 3)</i>	240.5
NM_133523	<i>Matrix metalloproteinase 3 (stromelysin 1, progelatinase)</i>	171.3
NM_013080	<i>Protein tyrosine phosphatase, receptor-type, Z polypeptide 1</i>	148.1
X73371	<i>Fc fragment of IgG, low affinity IIb, receptor (CD32)</i>	121.1
NM_012513	<i>Brain-derived neurotrophic factor</i>	106.2
NM_133298	<i>Glycoprotein (transmembrane) nmb</i>	94.4
AW528743	<i>Major histocompatibility complex, class II, DQ <math>\alpha</math>1</i>	91.1
AJ249701	<i>RT1 class Ib, locus Aw2</i>	77.2
BI290559	<i>Microsomal glutathione S-transferase 2</i>	74.5
AI176732	<i>Triggering receptor expressed on myeloid cells 2</i>	72.5
NM_030845	<i>Chemokine (C-X-C motif) ligand 2</i>	60.1
NM_023021	<i>Potassium intermediate/small conductance calcium-activated channel, subfamily N, member 4</i>	59.3
BF545627	<i>Ets variant gene 4 (E1A enhancer binding protein, E1AF)</i>	58.5
NM_012912	<i>Activating transcription factor 3</i>	53.8
AF065147	<i>CD44 antigen (homing function and Indian blood group system)</i>	53.8
AF268593	<i>Integrin, <math>\alpha</math>M</i>	50.6
AW527269	<i>Laminin, <math>\gamma</math>2</i>	49.5
Genes down-regulated in metastatic RCCs		
NM_052802	<i>Kidney androgen regulated protein</i>	3929.1
X04280	<i>Calbindin 1, 28 kDa</i>	1398.8
NM_017082	<i>Uromodulin (uromucoid, Tamm-Horsfall glycoprotein)</i>	1389.2
D13906	<i>Aquaporin 2 (collecting duct)</i>	1296.1
AB013455	<i>Solute carrier family 34 (sodium phosphate), member 1</i>	855.1
NM_013097	<i>Deoxyribonuclease I</i>	530.1
AI235942	<i>Aquaporin 4</i>	519.1
AI072107	<i>Aldo-keto reductase family 1, member C2</i>	471.1
BG377322	<i>Serpine peptidase inhibitor, clade C, member 1</i>	451.9
NM_012522	<i>cystathionine-<math>\beta</math>-synthase</i>	337.8
L29403	<i>Potassium inwardly-rectifying channel, subfamily J, member 1</i>	313.0
NM_017081	<i>Hydroxysteroid (11-<math>\beta</math>) dehydrogenase 2</i>	294.1
BE101119	<i>Parathyroid hormone receptor 1</i>	284.0
M27883	<i>Serine peptidase inhibitor, Kazal type 1</i>	270.6
NM_012619	<i>Phenylalanine hydroxylase</i>	265.0
NM_012842	<i>Epidermal growth factor (<math>\beta</math>-urogastrone)</i>	252.5
AA858962	<i>Retinol binding protein 4, plasma</i>	209.4
NM_031543	<i>Cytochrome P450, family 2, subfamily E, polypeptide 1</i>	199.5
NM_017111	<i>Solute carrier family 21, member 1</i>	186.1
BE097583	<i>Protein phosphatase 1, regulatory subunit 1A</i>	171.3

(clone 12; 1:100; BD Biosciences, San Jose, CA),  $\beta$ -catenin (clone 14; 1:100), phosphotyrosine (06-427; 1:100; Upstate, Lake Placid, NY), phospho- $\beta$ -catenin (Ser33/37/Thr41; 1:1000; Cell Signaling Technology, Danvers, MA), and proliferating cell nuclear antigen (clone PC10; 1:3000; BioGenex, San Ramon, CA).

### Immunohistochemistry and Immunocytochemistry

This was performed as previously described<sup>22</sup> with minor modifications. For the immunohistochemistry of paraffin-embedded specimens, the following antibodies were used:  $\beta$ -catenin (clone 196621; 1:100; R&D Systems, Inc., Minneapolis, MN), c-myc (clone 9E10; 1:50; Santa Cruz Biotechnology, Inc., Santa Cruz, CA), and cyclin D1 (SP4; 1:50; NeoMarkers, Inc., Fremont, CA). Antigen retrieval was performed by autoclaving at 121°C for 15 minutes in 10 mmol/L citrate buffer at pH 6.0. For the

immunocytochemistry, cells grown on Lab-Tek II Chamber Slide w/Cover (Nalge Nunc International, Naperville, IL) at approximately 70% confluence were fixed with cold methanol for 10 minutes, followed by permeation with 0.5% Triton X-100 for 10 minutes at room temperature. The same antibody against  $\beta$ -catenin was used at a dilution of 1:100. A tyramide signal amplification biotin system (PerkinElmer) was used to increase sensitivity. FITC-avidin and nuclear counterstaining with propidium iodide were used. Images were analyzed with confocal laser microscopy (Fluoview, Olympus, Osaka, Japan).

### Cell Proliferation Analysis

Cells were seeded in a six-well plate at first in Dulbecco's modified Eagle's medium with serum but without antibiotics. After 24 hours, siRNA oligonucleotides for *ptpr1* were transfected, followed by cell counting starting from 24 hours after transfection to the fifth day in triplicate.

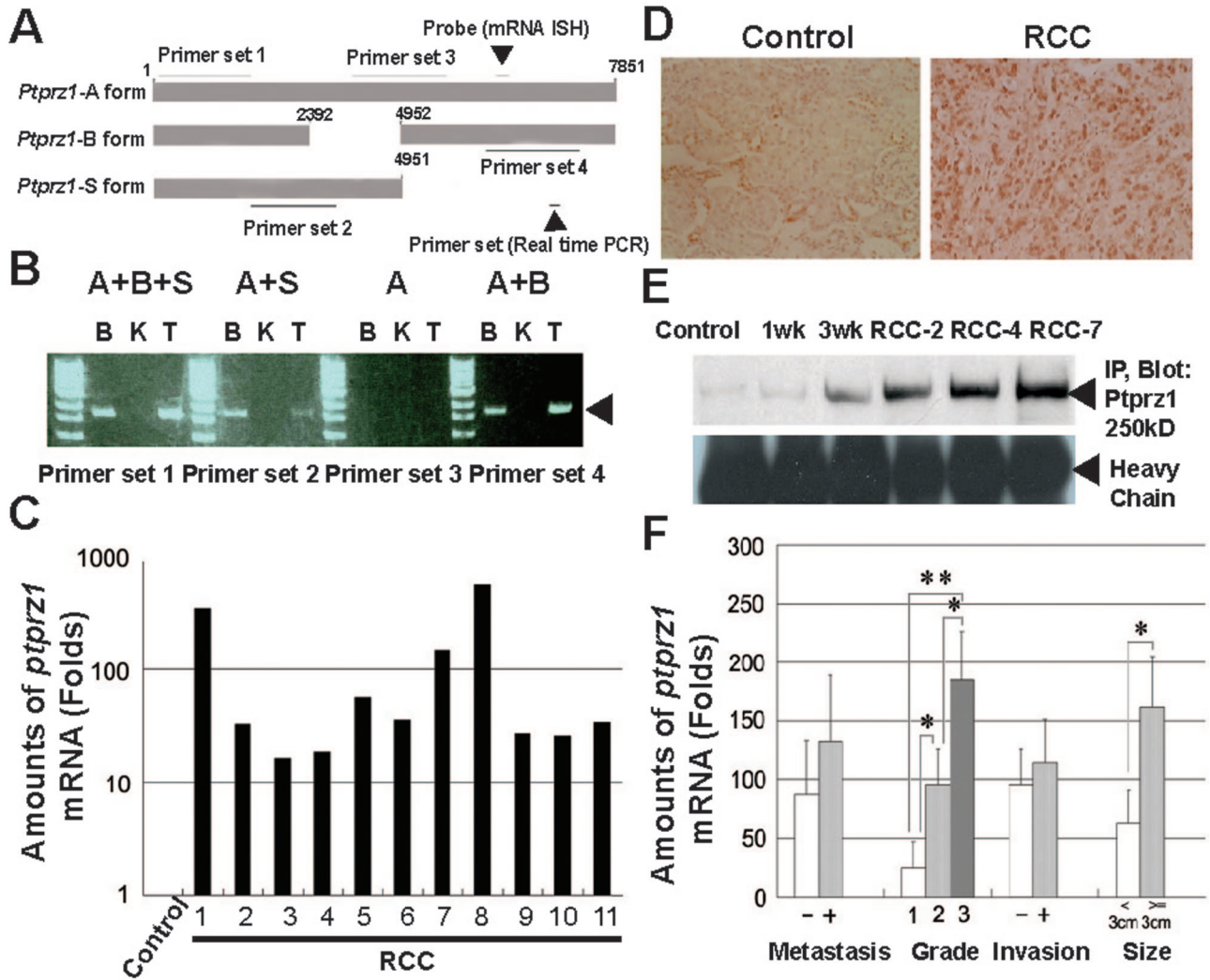


**Figure 2.** PTPRZ1 Isoform B is major in Fe-NTA-induced RCCs and is associated with tumor grade and size. **A:** Location of primers and mRNA hybridization probes in the *ptprz1* cDNA. Primer set 1 is common to all of the isoforms (A, B, and S); primer set 2 is specific to A and S isoforms; primer set 3 is specific only to A isoform; primer set 4 is specific to A and B isoforms. **B:** RT-PCR analysis. B, brain; K, control kidney; T, Fe-NTA-induced RCC. Control kidney expressed undetectable amount of *ptprz1* mRNA; major isoform in RCC was B isoform. A representative analysis is shown. **C:** Levels of *ptprz1* expression. Registered numbers of RCCs in Figure 1B and C and **E** in this figure correspond to each other. Means are shown after triplicate measurements that showed within 11% difference. Control, normal untreated kidney. **D:** mRNA is situ hybridization analysis. RCC cells expressed abundant *ptprz1* mRNA whereas control renal proximal tubules showed faint expression (original magnification,  $\times 80$ ). **E:** Protein levels of *ptprz1*. For specific and sensitive detection, immunoprecipitation was performed. Fe-NTA-induced RCCs as well as kidney after chronic oxidative stress by Fe-NTA for 3 weeks showed induction of PTPRZ1. **F:** Association of *ptprz1* mRNA levels with tumor parameters. Tumor grade and size revealed a proportional association with *ptprz1* expression (means  $\pm$  SEM,  $N = 3-10$ ; \* $P < 0.05$ ; \*\* $P < 0.01$ ).

### Statistical Analysis

Statistical analyses were performed with an unpaired *t*-test in which  $P < 0.05$  was considered as statistically significant.

### Results

#### Array-Based CGH and Gene Expression Microarray Analyses Identified *ptprz1* Amplification and Overexpression

We analyzed 13 Fe-NTA-induced rat RCCs and 2 cell lines established from them with array-based comparative genomic hybridization analyses. Chromosome

4q22 revealed the highest incidence of common genomic amplification among the 20 autosomes and X chromosome (Figure 1A). Detailed reports of the whole CGH analyses will be published elsewhere (S. Akatsuka and S. Toyokuni, unpublished data). At the same time, we analyzed four primary RCCs (two nonmetastatic and two metastatic tumors) with gene expression microarray analyses (Tables 1 and 2; Gene Expression Omnibus accession number GSE7625). With the expression microarray analyses, *ptprz1* was the fifth and sixth in the lists of up-regulated genes in nonmetastatic and metastatic RCCs, respectively, and was present on chromosome 4q22. Thus, we decided to focus on *ptprz1* based on these two sets of data. Quantitative PCR analyses revealed that 7 of 11 primary RCCs

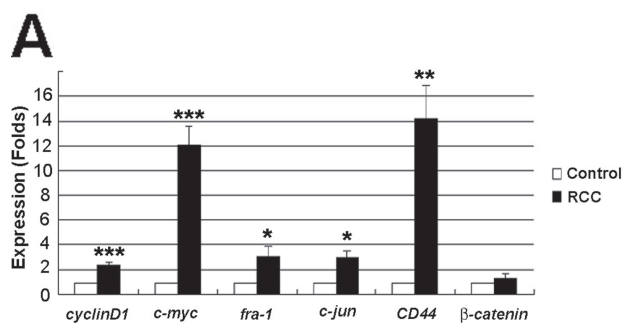
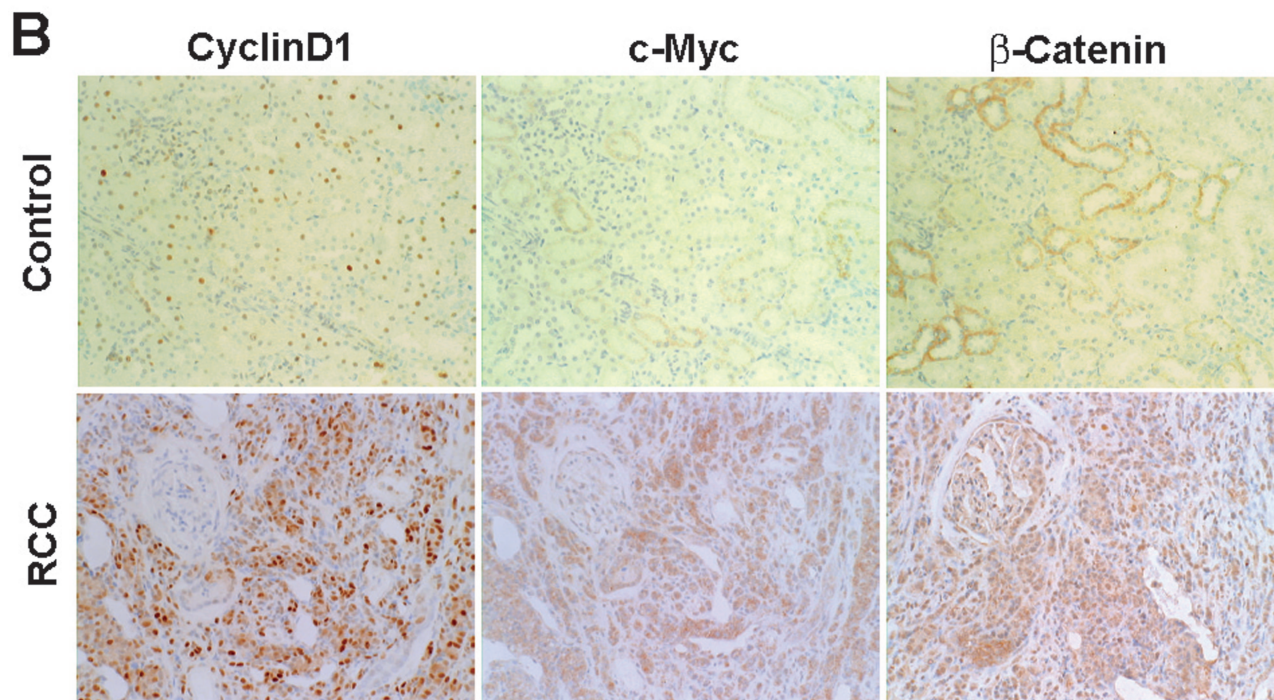


**Figure 3.**  $\beta$ -Catenin downstream genes are activated in Fe-NTA-induced RCCs. **A:** Expression of  $\beta$ -catenin downstream genes in Fe-NTA-induced RCCs measured by quantitative PCR analysis. All of the five genes revealed significantly elevated expression, whereas expression of  $\beta$ -catenin was not significantly changed. Control, normal untreated kidney (means  $\pm$  SEM,  $N = 3$ ; \* $P < 0.05$ ; \*\* $P < 0.01$ ; \*\*\* $P < 0.001$ ). **B:** Immunohistochemical analysis of  $\beta$ -catenin, *c-myc*, and cyclin D1. Weak immunostaining of  $\beta$ -catenin was observed in the distal tubules of normal kidney, whereas RCC showed moderate immunopositivity in the cytoplasm and in the nuclei, suggesting that  $\beta$ -catenin translocation may play an important role in the downstream regulation. RCC revealed moderate immunopositivity of *c-myc* and strong nuclear immunopositivity for cyclin D1. Representative images are shown. Control, normal untreated kidney. Specimens for control and RCC are serial sections, respectively. Refer to results for details (original magnification,  $\times 80$ ).



showed genomic amplification of *ptprz1* with 5 tumors showing more than fourfold increase (Figure 1B). We used fluorescence *in situ* hybridization analyses to confirm the amplification. In high-copy number tumors, a significantly increased number of signals were observed, whereas control cells showed two or less. Data obtained from cell lines were clearer because of the optimal fixation (Figure 1C).

### Overexpression of *ptprz1* Is Mainly of the B Isoform and Is Associated with Tumor Grade and Size

To differentiate three isoforms of *ptprz1* reported,<sup>24</sup> we designed specific primers for RT-PCR analyses (Figure 2A) and found that the B isoform is the major isoform in tumors (Figure 2B). Thus, we focused on the B isoform. All of the primary RCCs examined showed 16~552-fold increases in *ptprz1* expression in comparison with that of a normal untreated kidney (Figure 2C). *In situ* hybridization analyses confirmed the results, revealing abundant staining in the cytoplasm of RCC cells (Figure 2D). At the

protein level, repeated treatment of Fe-NTA for 3 weeks increased PTPRZ1 with a further increase in tumors (Figure 2E). We compared four parameters (pulmonary metastasis, grade, peritoneal invasion and tumor size) of the primary RCCs with mRNA levels and found that morphological grade<sup>13</sup> and size of the tumor were proportionally associated (Figure 2F).

### Overexpression of *ptprz1* Activates $\beta$ -catenin Pathway

Because network analysis of gene expression microarray data pointed out the involvement of the  $\beta$ -catenin signaling pathway, we studied the status of  $\beta$ -catenin and its downstream genes such as *cyclinD1*, *c-jun*, *c-myc*, *fra-1*, and *CD44* with quantitative PCR and immunohistochemistry. In the Fe-NTA-induced RCCs analyzed, all of the five  $\beta$ -catenin downstream genes were overexpressed, whereas  $\beta$ -catenin expression was not significantly increased (Figure 3A). Paraffin-embedded specimens were used for immunohistochemistry. Weak immunostaining of  $\beta$ -catenin was observed in the distal tubules of

normal kidney but not in the proximal tubules where Fe-NTA-induced RCCs are believed to be originated, whereas RCCs showed moderate immunopositivity in the cytoplasm and weak to moderate immunopositivity in the nuclei, suggesting that  $\beta$ -catenin abundance and translocation may play an important role in the downstream regulation. RCCs revealed weak to moderate immunopositivity of *c-myc*, and all of the RCCs showed strong nuclear immunopositivity for cyclin D1 (Figure 3B). These results strongly indicated the involvement of  $\beta$ -catenin pathway in the molecular mechanism of Fe-NTA-induced renal carcinogenesis. To demonstrate the causal relationship of *ptprz1* and  $\beta$ -catenin-downstream genes, we used cell culture systems thereafter.

Firstly, we evaluated the interaction of PTPRZ1 and  $\beta$ -catenin by the use of a nontransformed rat renal tubular cell line (NRK52E) and two Fe-NTA-induced rat RCC cell lines (FRCC-001 and FRCC-562).<sup>21</sup> We observed the presence of PTPRZ1 and the interaction of the two proteins only in the RCC cell lines (Figure 4A). Next, we performed *ptprz1* transfection to NRK52E cells and found that nuclear dephosphorylated  $\beta$ -catenin was significantly increased and that tyrosine, but not serine/threonine, residues were the target amino acid for dephosphorylation (Figure 4, B and C). This was accompanied by the expressional increase in the  $\beta$ -catenin downstream target genes such as *cyclinD1*, *c-jun*, *c-myc*, *fra-1*, and *CD44*, which was abolished with the simultaneous transfection of  $\beta$ -catenin siRNA, demonstrating that PTPRZ1 is upstream of  $\beta$ -catenin (Figure 5A). Furthermore, we performed an siRNA transfection study of *ptprz1* in the two RCC cell lines. With this procedure, nuclear  $\beta$ -catenin was significantly decreased with a relative increase in phosphorylated  $\beta$ -catenin at tyrosine (Figure 4B). This was accompanied by a marked expressional decrease in the  $\beta$ -catenin target genes (Figure 5, B and C). As seen by the nuclear presence of unphosphorylated  $\beta$ -catenin and the expressional increase in  $\beta$ -catenin downstream target genes, the endpoints were associated with cell proliferation and the levels of proliferating cell nuclear antigen (Figure 5, D–G).

### Discussion

The biological significance of oxidative stress resulting from the continuous consumption of oxygen has become more and more important with respect to the increase in human lifetime. Oxidative stress can induce two completely different outcomes depending on the extent and the situation, namely cell death or proliferation.<sup>30,31</sup> Cancer, one of the major causes of mortalities in the world, may be interpreted as a futile evolutionary effort on cellular proliferation under the given environment. Here, we undertook to obtain the responsible genetic alterations during carcinogenesis out of the selective process via chronic oxidative stress. In the established animal model of oxidative stress-induced carcinogenesis,<sup>5,12,32</sup> we found for the first time that oxidative stress amplifies certain specific chromosomal regions *in vivo* using array-based comprehensive CGH analysis.

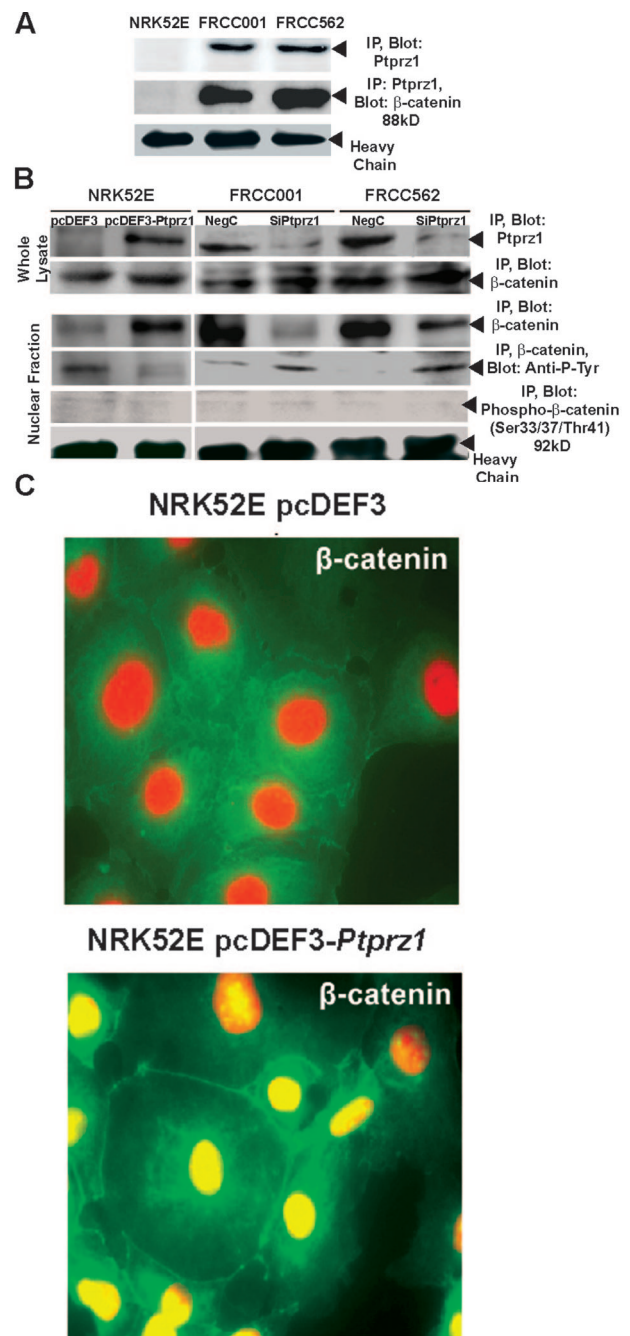


**Figure 4.** PTPRZ1 dephosphorylates tyrosine residues of  $\beta$ -catenin for nuclear translocation. **A:** Interaction of PTPRZ1 and  $\beta$ -catenin. NRK52E, non-transformed rat renal tubular cell line; FRCC-001 and FRCC-562 cell lines established from Fe-NTA-induced rat RCCs. PTPRZ1 is overexpressed only in FRCC cell lines and is associated with  $\beta$ -catenin. **B:** Tyrosine, but not serine or threonine, residues of  $\beta$ -catenin are the substrate of PTPRZ1 in association with nuclear translocation of  $\beta$ -catenin. **C:** Transfection of *ptprz1* induces nuclear translocation of  $\beta$ -catenin (fluorescein isothiocyanate; nuclear counterstaining by propidium iodide; original magnification,  $\times 400$ ).

Previously, Hunt et al<sup>33</sup> reported that chronic exposure of HA1 fibroblasts to increasing concentrations of H<sub>2</sub>O<sub>2</sub> or O<sub>2</sub> causes *catalase* gene amplification with increased amounts of message and protein and also discussed the results in association with the resistance against chemotherapeutic drugs in which pharmacological effects depend on oxidative stress. Our present findings are dis-



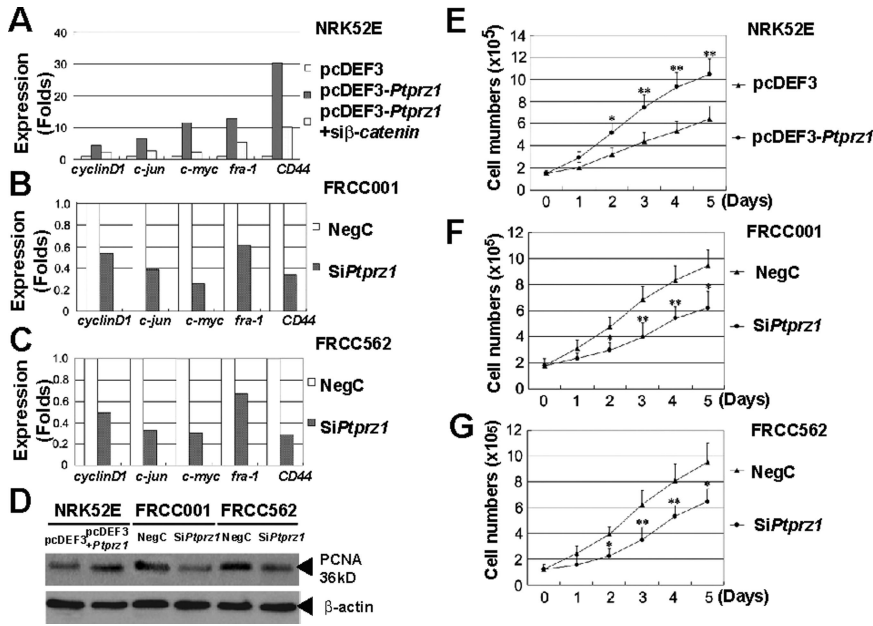


**Figure 5.** Function of  $\beta$ -catenin is regulated by *ptprz1*. **A–C:** Expression of  $\beta$ -catenin downstream genes is dependent on the levels of *ptprz1* expression. In NRK52E cells (**A**), transfection of *ptprz1* caused induction of  $\beta$ -catenin downstream genes, and this was reversed by specific knockdown of  $\beta$ -catenin. In FRCC-001 (**B**) and FRCC-562 (**C**) cells, specific knockdown of *ptprz1* caused down-regulation of  $\beta$ -catenin downstream genes. In **A–C**, means are shown after duplicate measurements that showed within 12% difference. **D:** Expressional levels of *ptprz1* are associated with protein levels of proliferating nuclear antigen (PCNA), a marker of cell proliferation. **E–G:** Expression levels of *ptprz1* are associated with cell proliferation. NegC, negative control (means  $\pm$  SEM,  $N = 3$ ; \* $P < 0.05$ , \*\* $P < 0.01$ ).

tinct from theirs in the following contexts: 1) gene amplification occurred in nonimmortalized cells *in vivo* at multiple different locations, suggesting either the presence of episomal/double minute chromosomes or multiple integration, and 2) the amplified genes were not necessarily associated with resistance to chronic oxidative stress. This is of note, considering the fact that a certain population of human cancers presents gene amplification, including the HER-2/neu proto-oncogene in breast cancers.<sup>34,35</sup> The results indicate that persistent oxidative stress is one of the driving forces for gene amplification.

We have integrated the results from CGH analysis and gene expression microarray analysis and focused on *ptprz1* (also called protein tyrosine phosphatase  $\zeta$  or receptor protein tyrosine phosphatase  $\beta$ ) in the present study. All of the 13 Fe-NTA-induced RCCs and two cell lines showed overexpression of *ptprz1*, whereas approximately one-half of them acquired gene amplification. Overexpression of *ptprz1* was observed after as early as 3 weeks of persistent oxidative stress. These results suggest that overexpression and the possible associated open chromatin structure are necessary but probably not enough for the gene amplification. Other possible factors involved are neighbor gene effect and chromosome territory. It is now believed that genomic DNA corresponding to certain chromosomes shares a rather fixed stereographical position in nuclei even in interphase.<sup>36,37</sup> Thus, a three-dimensional understanding of the neighboring genes would be necessary to understand fully the mechanism of gene amplification. Recently, we found that there are fragile sites (oxidative DNA base modifications) against oxidative stress in the genome using a novel method of DNA immunoprecipitation.<sup>15</sup> Genome replication, repair, and recombination should further be considered to elucidate the gene-amplifying mechanism. This carcinogenesis model presents an ideal material for further investigation.

We performed functional analyses on *ptprz1* expression using an untransformed rat renal tubular cell line and two cell lines derived from Fe-NTA-induced rat RCCs. *Ptpz1* mRNA was abundantly expressed in the cerebrum and cerebellum in rats but was extremely low in the heart, lung, liver, kidney, and stomach (approximately 1/100; data not shown). The major isoform of *ptprz1* in this model was the B isoform, one of the major isoforms in adult brain,<sup>24</sup> and chronic oxidative stress increased the expression of *ptprz1* in the kidney. So far, we have not yet identified the core consensus sequences in the promoter region of *ptprz1* that responded to chronic oxidative stress, but hypoxia-inducible factor-2 could be involved in this process because recent study suggested that hypoxia-inducible factor-2 overexpression is important in the development of renal carcinoma in patients with von Hippel Lindau tumor suppressor protein.<sup>38,39</sup> The A isoform was present during the prenatal period of rat brain and decreased rapidly after birth. Isoform B is the most deficient in the modification with carbohydrates among the three forms but retains cytoplasmic phosphatase domain.<sup>24</sup> With this information, we decided to identify the signal pathways involved downstream of the B isoform.

We focused on the  $\beta$ -catenin pathway because network analysis of the gene expression microarray data on RCCs indicated the involvement of this pathway. The  $\beta$ -catenin transcription coactivator is a key transducer of the Wnt signaling in the canonical pathway. In the absence of Wnt, a multiprotein destruction complex containing glycogen synthetase  $\beta$ , axin, disheveled, casein kinase 1, and adenomatous polyposis coli facilitates  $\beta$ -catenin degradation by the proteasome.<sup>40</sup> In our results, we add a novel switching mechanism of this pathway.

In the previous reports, function of *ptprz1* in cancer has been controversial. Meng et al reported that pleiotrophin,<sup>41</sup> a platelet-derived growth factor-inducible cytokine and a proto-oncogene, interacts with PTPRZ1 in a

glioblastoma cell line (U373-MG) to inactivate its catalytic activity, leading to an increase in the tyrosine phosphorylation levels of  $\beta$ -catenin.<sup>42</sup> In contrast, it was recently reported that targeting of PTPRZ1 with a monoclonal antibody delays tumor growth in a glioblastoma model.<sup>43,44</sup> We found that modulation of tyrosine phosphorylation in  $\beta$ -catenin controlled by *ptprz1* is a key process of the  $\beta$ -catenin pathway in this model. Activation of neither pleiotrophin nor Wnt signaling (Wnt2b, Wnt4, or Wnt5a) was observed (GEO accession number GSE7625; data not shown), but  $\beta$ -catenin was translocated to the nucleus, and the downstream target genes of  $\beta$ -catenin were activated in this model. This type of activation appears to be cell specific, considering the fact that normal renal proximal tubular cells show undetectable levels of *ptprz1* mRNA. *Ptporz1* has recently been identified as important in the recovery from demyelinating lesions,<sup>45</sup> is associated with susceptibility to VacA of *Helicobacter pylori* in murine stomach,<sup>46</sup> and was up-regulated after hypoxia-inducible factor-2 $\alpha$  transfection in HEK293T (adenovirus-transformed human fetal kidney cells).<sup>47</sup> It is possible to interpret from our results that cancer cells use metabolisms similar to fetal tissues in that they proliferate rapidly in a hypoxic environment.<sup>48</sup> 2-<sup>18</sup>F-fluoro-2-deoxy-D-glucose, a radioactive derivative of glucose, is widely used for the diagnosis of cancer, based on the increased glucose consumption of cancer cells.<sup>49</sup> Our previous observation in this carcinogenesis model that thioredoxin-binding protein-2 is inactivated via methylation of the promoter region, leading to the activation of glycolytic pathway via thioredoxin system,<sup>22,50</sup> supports this hypothesis.

In conclusion, we show for the first time, to our knowledge, that chronic oxidative stress causes gene amplification *in vivo* through a combination of comprehensive array-based CGH and gene expression microarray analyses in an oxidative stress-induced carcinogenesis model. Furthermore, we found a novel  $\beta$ -catenin signal activation mechanism through overexpression of *ptprz1* protein tyrosine phosphatase. Oxidative stress is closely associated not only with carcinogenesis but also with tumor biology.<sup>10,31</sup> We believe that oxidative stress, especially of a chronic nature, presents an environment for competitive cell proliferation rather than cooperative cell survival, giving opportunities for selection. We do not know at present whether activation of the  $\beta$ -catenin pathway through *ptprz1* amplification is a specific event only in renal tubular cells or oxidative stress-induced carcinogenesis. Because gene amplification in human cancer is often associated with poor prognosis<sup>51</sup> and is a mechanism of resistance to therapies,<sup>52</sup> this animal model confers an intriguing opportunity not only for the elucidation of carcinogenesis toward cancer prevention but also of therapeutic resistance.

### Acknowledgments

We thank Dr. Masaharu Noda (National Institute for Basic Biology, Okazaki, Japan) for discussion. The pcDEF3 expression vector was a kind gift from Dr. Gerome A Langer (Robert Wood Johnson Medical School, Piscataway, NJ).

### References

- Halliwell B, Gutteridge JMC: Free Radicals in Biology and Medicine. New York, Oxford University Press, 2007
- Iuchi K, Ichimiya A, Akashi A, Mizuta T, Lee Y, Tada H, Mori T, Sawamura K, Lee Y, Furuse K, Yamamoto S, Aozasa K: Non-Hodgkin's lymphoma of the pleural cavity developing from long-standing pyothorax. *Cancer* 1987, 60:1771-1775
- Uemura N, Okamoto S, Yamamoto S, Matsumura N, Yamaguchi S, Yamakido M, Taniyama K, Sasaki N, Schlemper R: *Helicobacter pylori* infection and the development of gastric cancer. *N Engl J Med* 2001, 345:784-789
- Eaden J, Abrams K, Mayberry J: The risk of colorectal cancer in ulcerative colitis: a meta-analysis. *Gut* 2001, 48:526-535
- Toyokuni S: Iron-induced carcinogenesis: the role of redox regulation. *Free Radic Biol Med* 1996, 20:553-566
- Elmberg M, Hultcrantz R, Ekblom A, Brandt L, Olsson S, Olsson R, Lindgren S, Loof L, Stal P, Wallerstedt S, Almer S, Sandberg-Gertzen H, Askling J: Cancer risk in patients with hereditary hemochromatosis and in their first-degree relatives. *Gastroenterology* 2003, 125:1733-1741
- Hodgson J, Darnton A: The quantitative risks of mesothelioma and lung cancer in relation to asbestos exposure. *Ann Occup Hyg* 2000, 44:565-601
- Nishigori C, Hattori Y, Toyokuni S: Role of reactive oxygen species in skin carcinogenesis. *Antioxid Redox Signal* 2004, 6:561-570
- Preston D, Kusumi S, Tomonaga M, Izumi S, Ron E, Kuramoto A, Kamada N, Dohy H, Matsui T, Nonaka H, Thompson DE, Soda M, Mabuchi K: Cancer incidence in atomic bomb survivors: Part III. Leukemia, lymphoma and multiple myeloma, 1950-1987. *Radiat Res* 1994, 137:S68-S97
- Toyokuni S, Okamoto K, Yodoi J, Hiai H: Persistent oxidative stress in cancer. *FEBS Lett* 1995, 358:1-3
- Li JL, Okada S, Hamazaki S, Ebina Y, Midorikawa O: Subacute nephrotoxicity and induction of renal cell carcinoma in mice treated with ferric nitrilotriacetate. *Cancer Res* 1987, 47:1867-1869
- Ebina Y, Okada S, Hamazaki S, Ogino F, Li JL, Midorikawa O: Nephrotoxicity and renal cell carcinoma after use of iron- and aluminum-nitrilotriacetate complexes in rats. *J Natl Cancer Inst* 1986, 76:107-113
- Nishiyama Y, Suwa H, Okamoto K, Fukumoto M, Hiai H, Toyokuni S: Low incidence of point mutations in H-, K- and N-ras oncogenes and p53 tumor suppressor gene in renal cell carcinoma and peritoneal mesothelioma of Wistar rats induced by ferric nitrilotriacetate. *Jpn J Cancer Res* 1995, 86:1150-1158
- Toyokuni S, Mori T, Dizdaroglu M: DNA base modifications in renal chromatin of Wistar rats treated with a renal carcinogen, ferric nitrilotriacetate. *Int J Cancer* 1994, 57:123-128
- Akatsuka S, Aung TT, Dutta KK, Jiang L, Lee WH, Liu YT, Onuki J, Shirase T, Yamasaki K, Ochi H, Naito Y, Yoshikawa T, Kasai H, Tominaga Y, Sakumi K, Nakabeppu Y, Kawai Y, Uchida K, Yamasaki A, Tsuruyama T, Yamada Y, Toyokuni S: Contrasting genome-wide distribution of 8-hydroxyguanine and acrolein-modified adenine during oxidative stress-induced renal carcinogenesis. *Am J Pathol* 2006, 169:1328-1342
- Toyokuni S, Uchida K, Okamoto K, Hattori-Nakakuki Y, Hiai H, Stadtman ER: Formation of 4-hydroxy-2-nonenal-modified proteins in the renal proximal tubules of rats treated with a renal carcinogen, ferric nitrilotriacetate. *Proc Natl Acad Sci USA* 1994, 91:2616-2620
- Toyokuni S, Luo XP, Tanaka T, Uchida K, Hiai H, Lehotay DC: Induction of a wide range of C<sub>2-12</sub> aldehydes and C<sub>7-12</sub> acylolins in the kidney of Wistar rats after treatment with a renal carcinogen, ferric nitrilotriacetate. *Free Radic Biol Med* 1997, 22:1019-1027
- Zhang D, Okada S, Yu Y, Zheng P, Yamaguchi R, Kasai H: Vitamin E inhibits apoptosis: DNA modification, and cancer incidence induced by iron-mediated peroxidation in Wistar rat kidney. *Cancer Res* 1997, 57:2410-2414
- Tanaka T, Iwasa Y, Kondo S, Hiai H, Toyokuni S: High incidence of allelic loss on chromosome 5 and inactivation of p15<sup>INK4B</sup> and p16<sup>INK4A</sup> tumor suppressor genes in oxystress-induced renal cell carcinoma of rats. *Oncogene* 1999, 18:3793-3797
- Hiroyasu M, Ozeki M, Kohda H, Echizenya M, Tanaka T, Hiai H, Toyokuni S: Specific allelic loss of p16<sup>INK4A</sup> tumor suppressor gene

- after weeks of iron-mediated oxidative damage during rat renal carcinogenesis. *Am J Pathol* 2002, 160:419–424
21. Tanaka T, Akatsuka S, Ozeki M, Shirase T, Hiai H, Toyokuni S: Redox regulation of annexin 2 and its implications for oxidative stress-induced renal carcinogenesis and metastasis. *Oncogene* 2004, 23:3980–3989
  22. Dutta KK, Nishinaka Y, Masutani H, Akatsuka S, Aung TT, Shirase T, Lee W-H, Hiai H, Yodoi J, Toyokuni S: Two distinct mechanisms for loss of thioredoxin-binding protein-2 in oxidative stress-induced renal carcinogenesis. *Lab Invest* 2005, 85:798–807
  23. Lee W, Akatsuka S, Shirase T, Kumar Dutta K, Jiang L, Liu Y, Onuki J, Yamada Y, Okawa K, Wada Y, Watanabe A, Kohro T, Noguchi N, Toyokuni S:  $\alpha$ -Tocopherol induces calnexin in renal tubular cells: another protective mechanism against free radical-induced cellular damage. *Arch Biochem Biophys* 2006, 453:168–178
  24. Nishiwaki T, Maeda N, Noda M: Characterization and developmental regulation of proteoglycan-type protein tyrosine phosphatase zeta/RPTPbeta isoforms. *J Biochem (Tokyo)* 1998, 123:458–467
  25. Yamamoto-Fukuda T, Aoki D, Hishikawa Y, Kobayashi T, Takahashi H, Koji T: Possible involvement of keratinocyte growth factor and its receptor in enhanced epithelial-cell proliferation and acquired recurrence of middle-ear cholesteatoma. *Lab Invest* 2003, 83:123–136
  26. Hattori Y, Nishigori C, Tanaka T, Uchida K, Nikaido O, Osawa T, Hiai H, Imamura S, Toyokuni S: 8-Hydroxy-2'-deoxyguanosine is increased in epidermal cells of hairless mice after chronic UVB exposure. *J Invest Dermatol* 1996, 107:733–737
  27. Goldman L, Cutrone E, Kotenko S, Krause C, Langer J: Modifications of vectors pEF-BOS, pcDNA1 and pcDNA3 result in improved convenience and expression. *Biotechniques* 1996, 21:1013–1015
  28. Naito Y, Yamada T, Ui-Tei K, Morishita S, Saigo K: siDirect: highly effective, target-specific siRNA design software for mammalian RNA interference. *Nucleic Acids Res* 2004, 32:W124–W129
  29. Toyokuni S, Kawaguchi W, Akatsuka S, Hiroyasu M, Hiai H: Intermittent microwave irradiation facilitates antigen-antibody reaction in Western blot analysis. *Pathol Int* 2003, 53:259–261
  30. Toyokuni S, Akatsuka S: What has been learned from the studies of oxidative stress-induced carcinogenesis: proposal of the concept of oxygenomics. *J Clin Biochem Nutr* 2006, 39:3–10
  31. Toyokuni S, Akatsuka S: Pathological investigation of oxidative stress in the postgenomic era. *Pathol Int* 2007, 57:461–473
  32. Okada S: Iron-induced tissue damage and cancer: the role of reactive oxygen free radicals. *Pathol Int* 1996, 46:311–332
  33. Hunt C, Sim J, Sullivan S, Featherstone T, Golden W, Von Kapp-Herr C, Hock R, Gomez R, Parsian A, Spitz D: Genomic instability and catalase gene amplification induced by chronic exposure to oxidative stress. *Cancer Res* 1998, 58:3986–3992
  34. Slamon D, Clark G, Wong S, Levin W, Ullrich A, McGuire W: Human breast cancer: correlation of relapse and survival with amplification of the HER-2/neu oncogene. *Science* 1987, 235:177–182
  35. Albertson D: Gene amplification in cancer. *Trends Genet* 2006, 22:447–455
  36. Cremer T, Cremer C: Chromosome territories, nuclear architecture and gene regulation in mammalian cells. *Nat Rev Genet* 2001, 2:292–301
  37. Meaburn KJ, Misteli T: Chromosome territories. *Nature* 2007, 445:379–381
  38. Maranchie J, Vasselli J, Riss J, Bonifacino J, Linehan W, Klausner R: The contribution of VHL substrate binding and HIF1- $\alpha$  to the phenotype of VHL loss in renal cell carcinoma. *Cancer Cell* 2002, 1:247–255
  39. Kondo K, Klco J, Nakamura E, Lechpammer M, Kaelin W: Inhibition of HIF is necessary for tumor suppression by the von Hippel-Lindau protein. *Cancer Cell* 2002, 1:237–246
  40. Clevers H: Wnt/beta-catenin signaling in development and disease. *Cell* 2006, 127:469–480
  41. Chauhan A, Li Y, Deuel T: Pleiotrophin transforms NIH 3T3 cells and induces tumors in nude mice. *Proc Natl Acad Sci USA* 1993, 90:679–682
  42. Meng K, Rodriguez-Pena A, Dimitrov T, Chen W, Yamin M, Noda M, Deuel T: Pleiotrophin signals increased tyrosine phosphorylation of beta-catenin through inactivation of the intrinsic catalytic activity of the receptor-type protein tyrosine phosphatase beta/zeta. *Proc Natl Acad Sci USA* 2000, 97:2603–2608
  43. Foehr E, Lorente G, Kuo J, Ram R, Nikolich K, Urfer R: Targeting of the receptor protein tyrosine phosphatase beta with a monoclonal antibody delays tumor growth in a glioblastoma model. *Cancer Res* 2006, 66:2271–2278
  44. Ulbricht U, Eckerich C, Fillbrandt R, Westphal M, Lamszus K: RNA interference targeting protein tyrosine phosphatase zeta/receptor-type protein tyrosine phosphatase beta suppresses glioblastoma growth in vitro and in vivo. *J Neurochem* 2006, 98:1497–1506
  45. Harroch S, Furtado G, Brueck W, Rosenbluth J, Lafaille J, Chao M, Buxbaum J, Schlessinger J: A critical role for the protein tyrosine phosphatase receptor type Z in functional recovery from demyelinating lesions. *Nat Genet* 2002, 32:411–414
  46. Fujikawa A, Shirasaka D, Yamamoto S, Ota H, Yahiro K, Fukada M, Shintani T, Wada A, Aoyama N, Hirayama T, Fukamachi H, Noda M: Mice deficient in protein tyrosine phosphatase receptor type Z are resistant to gastric ulcer induction by VacA of *Helicobacter pylori*. *Nat Genet* 2003, 33:375–381
  47. Wang V, Davis D, Haque M, Huang L, Yarchoan R: Differential gene up-regulation by hypoxia-inducible factor-1 $\alpha$  and hypoxia-inducible factor-2 $\alpha$  in HEK293T cells. *Cancer Res* 2005, 65:3299–3306
  48. Nodwell A, Carmichael L, Ross M, Richardson B: Placental compared with umbilical cord blood to assess fetal blood gas and acid-base status. *Obstet Gynecol* 2005, 105:129–138
  49. Endo K, Oriuchi N, Higuchi T, Iida Y, Hanaoka H, Miyakubo M, Ishikita T, Koyama K: PET and PET/CT using <sup>18</sup>F-FDG in the diagnosis and management of cancer patients. *Int J Clin Oncol* 2006, 11:286–296
  50. Oka S, Liu W, Masutani H, Hirata H, Shinkai Y, Yamada S, Yoshida T, Nakamura H, Yodoi J: Impaired fatty acid utilization in thioredoxin binding protein-2 (TBP-2)-deficient mice: a unique animal model of Reye syndrome. *FASEB J* 2005, 147:733–743
  51. Chung C, Ely K, McGavran L, Varela-Garcia M, Parker J, Parker N, Jarrett C, Carter J, Murphy B, Netterville J, Burkey B, Sinard R, Cmelak A, Levy S, Yarbrough W, Slebos R, Hirsch F: Increased epidermal growth factor receptor gene copy number is associated with poor prognosis in head and neck squamous cell carcinomas. *J Clin Oncol* 2006, 24:4170–4176
  52. Cullen K, Newkirk K, Schumaker L, Aldosari N, Rone J, Haddad B: Glutathione S-transferase pi amplification is associated with cisplatin resistance in head and neck squamous cell carcinoma cell lines and primary tumors. *Cancer Res* 2003, 63:8097–8102